Design optimization of a polygeneration plant producing power, heat, and lignocellulosic ethanol

Lythcke-Jørgensen, Christoffer Ernst; Haglind, Fredrik

Published in:
Energy Conversion and Management

Link to article, DOI:
10.1016/j.enconman.2014.12.028

Publication date:
2015

Document Version
Peer reviewed version

Design optimization of a polygeneration plant producing power, heat, and lignocellulosic ethanol

Christoffer Lythcke-Jørgensen[a]* Fredrik Haglind[b]

[a] Technical University of Denmark, Department of Mechanical Engineering, Nils Koppels Allé 403, DK-2800 Kgs. Lyngby, celjo@mek.dtu.dk

[b] Technical University of Denmark, Department of Mechanical Engineering, Nils Koppels Allé 403, DK-2800 Kgs. Lyngby, frh@mek.dtu.dk

* Corresponding author. +45 30 42 72 00. Email: celjo@mek.dtu.dk.

Abstract

A promising way to increase the energy efficiency and reduce costs of biofuel production is to integrate it with heat and power production in polygeneration plants. This study treats the retrofitting of a Danish combined heat and power plant by integrating lignocellulosic ethanol production based on wheat straw with the aim of minimizing specific ethanol production cost. Previously developed and validated models of the facilities are applied in the attempt to solve the design optimization problem. Straw processing capacities in the range of 5 kg/s to 12 kg/s are considered, while plant operation is optimized over the year with respect to maximal income and with the limitations that the reference hourly district heating production has to be met while reference hourly power export cannot be exceeded.

The results suggest that the specific ethanol production cost increased continuously from 0.958 Euro/L at a straw processing capacity of 5 kg/s to 1.113 Euro/L at a capacity of 12 kg/s, indicating that diseconomies-of-scale applies for the suggested ethanol production scheme. A thermodynamic evaluation further discloses that the average yearly exergy efficiency decreases continuously with increasing ethanol production capacity, ranging from 0.746 for 5 kg/s to 0.696 for 12 kg/s. This trend results from operating constraints that induce expensive operation patterns in periods of high district heating loads or shut-down periods for the combined heat and power plant. A sensitivity analysis indicates that the found optimum is indifferent to major variations in fossil fuel prices. The results question the efficiency of the suggested retrofitting scheme in the present energy system, and they further point towards the importance of taking operating conditions into consideration when developing flexible polygeneration plant concepts as differences between design-point operation and actual operation may have a significant impact on overall plant performance.

Keywords

Combined heat and power; design optimization; exergy efficiency; lignocellulosic ethanol; operation optimization; polygeneration

Nomenclature

Latin letters

C	Cost [Euro]
c	Specific cost [Euro/GJ]
D	Dimension [-]
$\dot{EX}$	Exergy flow [MJ/h]
ex	Specific exergy flow [MJ/kg]
I	Investment [Euro]

M	Mass [kg]
M_f	Capacity power factor [-]
$\dot{P}$	Power production [MW]
Q	Heat [MJ]
$\dot{Q}$	Heat flow [MJ/s]
$\dot{Q}_{fuel}$	Fuel input [MJ/s]
V_{eth}	Volume ethanol production [L/h]

Greek letters

α	Back-pressure operation parameter [-]
β	Relative district heating production in the ethanol facility [-]
η_{eth}	Mass efficiency of lignocellulosic-biomass-to-ethanol conversion [-]
η_{ex}	Standard exergy efficiency [-]
κ	Choice between integrated or separate operation [-]
λ	Combined heat and power unit load [-]
ρ	Density [kg/L]
σ	Straw processing capacity of the ethanol production [kg/s]

Subscripts

add	Additives
enz	Enzymes
eth	Ethanol
i	Hour of the year
I	Investment depreciation
$O\&M$	Operation and maintenance
ref	Reference production

0	Reference value

Abbreviations

AVV1	Avedøreværket 1
CHP	Combined Heat and Power
DH	District Heating
L&D	(Exergy) Losses and Destruction
O&M	Operation and Maintenance
SSF	Simultaneous Saccharification and Fermentation

1. Introduction

Biomass, being the only renewable resource of highly concentrated carbon, is often considered a cornerstone in renewable energy systems because of its storability and potential conversability to biofuels with high energy densities [1]. The biomass resource, however, is limited [2], and competition between food and energy production pose a sustainability challenge [3]. Efficient use and conversion of sustainably available biomass are therefore of crucial importance in renewable energy systems [4].

Among biofuels, ethanol is presently the most widely used for transportation on a global basis and it is consumed both as an individual fuel and in blends with gasoline [5]. Ethanol produced from lignocellulosic biomass is of special interest here because it may yield reduced CO_2 emissions from transportation without linking fuel prices and food prices directly [4]. Furthermore, ethanol is a bulk-volume chemical used in industrial and consumer products and lignocellulosic ethanol

presents a green chemistry [6][1] alternative to the existing ethanol production from ethene hydration or through fermentation of sugars and starch [7]. However, the energy intensive nature of lignocellulosic ethanol production is a challenge with respect to production efficiency and economy.

In an extensive work on the integrated production of biogas, heat and power based on biomass gasification, Gassner et Maréchal [8] concluded that biofuel plants may increase energy- and cost-efficiency simultaneously by applying process systems engineering approaches and by considering integration with other processes in polygeneration plants (PGPs). Similarly, a promising way to increase energy- and cost-efficiency of lignocellulosic ethanol production is to integrate it with heat and power production [4]. Plants integrating the production of power, heat, bio-methane, and lignocellulosic ethanol have been investigated by several groups, both as grassroot design problems and retrofit design problems. Regarding grassroot design problems, Daianova et al. [9] and Ilic et al. [10] both reported better energy economy for integrated PGPs compared to stand-alone production of the same energy products, assuming constant energy prices over the year. Bösch et al. [11] discussed how the energy economy of a system producing lignocellulosic ethanol, biogas and district heating (DH) might be increased by integrating power production. For a similar system, Modarresi et al. [12] conducted a pinch analysis and reported that heat integration can reduce the hot and cold utility demands by up to 40%, assuming operation in design point solely. Leduc et al. [13] conducted a sensitivity analysis of the important parameters for such systems in Sweden and found that incomes from heat and power sales were the most significant contributors towards reducing the specific ethanol production costs. With regard to retrofitted systems, Palacios-Bereche

[1] Green chemistry consists of environmental friendly, sustainable chemicals and processes the use of which results in reduced waste, safer outputs, and reduced or eliminated pollution and environmental damage [6].

et al. [14] studied the integration of lignocellulosic ethanol production in the conventional first-generation sugarcane ethanol process and reported higher exergy efficiency for the integrated scheme when considering only design point operation. Lythcke-Jørgensen et al. [15] investigated the introduction of lignocellulosic ethanol production in an existing combined heat and power (CHP) and also reported higher exergy efficiencies for integrated operation. In a study of conversion routes for winter wheat to ethanol, Bentsen et al. [16] suggested that energy savings could be achieved by integrating lignocellulosic ethanol production in existing CHP units. Starfelt et al. [17] investigated the integration of lignocellulosic ethanol production in an existing biomass-based CHP unit in Sweden and concluded that for the same production of heat, power, and ethanol, the total biomass consumption would be lower for the integrated system than for a separate scenario. And in a later study, Starfelt et al. [18] concluded that the integration of lignocellulosic ethanol production in Swedish CHP units with fixed heat-to-power ratios may be profitable if excess heat capacity is available in the CHP unit for a certain amount of time over the year.

In principle, the development and optimization of PGPs can be considered at three levels, similar to the optimization of energy systems [19] and distributed energy supply systems [20]: Synthesis level, design level, and operation level. At the synthesis level, the configuration of the PGP is optimized by either retrofitting an existing plant (retrofit design) or by developing a new plant concept (grassroot design)[2], which entails the selection of the desired products and processes. At the design level, one considers process dimensioning, process integration, required components, and technical specifications of the equipment. Finally, at the operation level, the operation mode of the given plant is optimized in the surrounding energy system; this is done by taking expected demands for, and costs of, energy services and utilities into account as well as interactions with other energy

[2] A grassroot design is *a priori* always a solution to a retrofit design optimization problem [20].

producers in the system. The operation level is especially important for flexible operating PGPs, e.g. those set to balance production from intermittent renewable energy sources [21] whenever economically advantageous [22]. Optimization on operation level has been investigated in literature for polygeneration plants producing power, heating, cold and fresh water, e.g. in a sequential optimization methodology presented by Uche et al. [23]. Grisi et al. [24] further illustrated how commodity market prices may affect operation decisions in a sugarcane biorefinery producing power, sugar, sugar- and bagasse-based ethanol, and biogas. However, to the authors' best knowledge the impact of flexible plant operation on economic performance has not been treated comprehensively in previous studies of the integrated production of power, heat, and lignocellulosic ethanol.

This study assesses the impact on economic and thermodynamic performance of integrating lignocellulosic ethanol production with flexible heat and power production. The study treats a retrofit design problem where lignocellulosic ethanol production using the hydrothermal pretreatment technology IBUS [25][3] is sought integrated into the Danish CHP unit Avedøreværket 1 (AVV1). The system has previously been studied by the authors and the outcomes suggested that operating conditions may have a significant impact on both economy [26] and overall exergy efficiency [27] [15] of the ethanol production. This work builds upon the previous study by optimizing the PGP at design and operation levels and simultaneously attempting to minimize the break-even specific ethanol production costs. For each solution to the design problem, the thermodynamic performance of the ethanol production is further evaluated by applying exergy analysis [28] and calculating the average exergy efficiency of the ethanol production over the year.

[3] IBUS (Integrated Biomass Utilization System) is a patented cellulosic biomass pretreatment technology. The patent is owned by the Danish company Inbicon A/S, a subsidiary to DONG Energy.

In this paper, the modelling approach and outcomes of previous studies are given in Section 2. The design optimization scheme and the thermodynamic performance evaluation method are presented in Section 3. The outcomes are presented in Section 4 and discussed in Section 5. Finally, Section 6 contains a conclusion of the findings.

2. System description and previous work

2.1. System description

The design optimization problem treated in this study concerns the integration of lignocellulosic ethanol production based on IBUS technology in the existing Danish combined heat and power unit Avedøreværket 1. A simplified layout of the PGP is presented in Figure 1. A thorough description of the plant synthesis and modelling, including choice of performance parameters and modelling validation, is presented in Lythcke-Jørgensen et al. [15].

Avedøreværket 1 (AVV1), which was commissioned in 1990, has a net electric power generation in condensation mode of 250 MW, and of 212 MW in full back pressure mode with a district heating (DH) production of 330 MJ/s (drive temperature/return temperature 100^0C/50^0C) [29]. Part-load operation in the CHP unit is governed by sliding-pressure control [30]. A numerical model of AVV1, developed by Elmegaard and Houbak [29] in the energy system simulator Dynamic Network Analysis [31], was used for simulating flows and operation of the CHP unit.

An ethanol production facility based on IBUS technology produces lignocellulosic ethanol, solid biofuel, and molasses from wheat straw. In the facility, the lignocellulosic structure of the straw is broken down through treatment with pressurized steam in the hydrothermal pretreatment stage, whereupon the straw-steam mixture is split into a fiber fraction and a liquid fraction. The fiber fraction is liquefied by glucose-forming enzymes before fermentation is initiated in simultaneous fermentation and saccharification (SSF) tanks. Ethanol is distilled from the resulting fermentation

broth, leaving a fiber stillage which is treated in various separation stages alongside the pretreatment liquid fraction, yielding a solid biofuel fraction, a molasses fraction, and a waste water fraction. The molasses fraction can be used in anaerobic fermentation to produce biogas [12] or as animal feed [32], while the solid biofuel can be used for combustion or gasification. A model of the ethanol facility based on heat and mass balances over each of the system processes was developed in the software Engineering Equation Solver (EES) [33] using the layout reported by Larsen et al. [32] and Østergaard Petersen et al. [34]. The flows of yeast and enzymes were neglected in mass balance calculations as they were found to be insignificant. The mass conversion efficiencies for the ethanol facility products are presented in Table 1.

2.2. Outcomes of previous work

In the previous studies of the polygeneration plant, a fixed design was applied to the system in which the ethanol facility was dimensioned to process all locally available winter wheat straw within a distance of 50 km from the plant, yielding a straw processing capacity of 6.22 kg/s all year round. Because of load transition times of more than 180 hours in the ethanol production facility [34], load changes and stop-and-go operation were not considered feasible and full-load operation was therefore assumed for the whole year. As the CHP unit was operated according to flexible power and heat demands, the ethanol production in the PGP could be run in two ways: Integrated mode or separate mode. In integrated mode, steam extracted from turbines of the CHP unit was used for covering the hot utility demand of the ethanol facility. During integrated operation, DH production from the IBUS facility was prioritized over DH production from the CHP unit. In separate mode, a natural gas boiler with a first law energy efficiency of $\eta_{boiler} = 0.96$ [35] was used for generating the steam required by the ethanol facility, and DH production in the ethanol facility was not considered. The principles of the two PGP operation modes are outlined in Figure 2.

In Lythcke-Jørgensen et al. [26], a combined pinch analysis [36] and exergy analysis [28] was carried out to identify the minimum hot and cold utility demands in the ethanol facility as well as the steam extraction pattern with the lowest exergy destruction during integrated mode operation. A 10K pinch temperature difference was used, as suggested by Modarresi et al. [12] for a similar facility. The resulting specific hot and cold utility demands and power consumption of the ethanol production per kilogram of biomass treated are presented in Table 2.

As regards existing steam extraction points in AVV1 only, the optimal integration solution involved steam extraction from the points marked (A), (B), and (C) in Figure 1. The thermodynamic states of steam in the three points are summarized in Table 3. Steam for hydrothermal pretreatment was extracted from node (B) in AVV1 at CHP loads above 0.6, and from node (A) at CHP loads below 0.6. The steam for hydrothermal pretreatment was conditioned in the heat integration network to meet the exact temperature and pressure requirements of the hydrothermal pretreatment component, 195°C and 13bar [37]. Heat released from steam conditioning was used internally in the ethanol facility. The remaining hot utility demand of the ethanol facility was covered by steam extracted from node (C). Condensate from the heat integration network is recycled to the condenser of AVV1 where additional desalinated water is added to compensate for the loss of steam to the hydrothermal pretreatment. Cooling in the heat integration network is provided by sea water and by DH water when DH production is activated in the ethanol facility.

The energy economy of the PGP was evaluated in Lythcke-Jørgensen et al. [26]. Considering the PGP as a substitute to AVV1 in the existing Danish energy system and assuming hour-wise quasi-static operation, the plant was set to produce the same hourly amounts of heat and power as the CHP unit delivered in 2011, the chosen reference year. Separate operation occurred in periods with high power demands where steam extraction for driving the ethanol production was not available and in periods where the CHP unit was shut down. The results suggested that on an average the

specific energy cost for the ethanol production could be more than eight times higher during separate operation than during integrated operation, and that it might be economically advantageous to optimize the operation pattern of the PGP towards a longer duration of integrated operation. A scatter distribution of the hour-wise quasi-static operation points for the reference operation is presented in Figure 3. It should be noted that separate operation occurred for 2060 hours of the year due to CHP shut-down.

Two other studies by Lythcke-Jørgensen et al. [27] [15] investigated six different operation points for the reference PGP and found that within these, the exergy efficiency of the ethanol production varied from 0.564 to 0.855. The highest exergy efficiency was obtained for integrated operation with full DH production in the ethanol facility and lowest possible load in the CHP unit, while the lowest exergy efficiency was obtained for separate operation. The reason for the large differences in exergy efficiency was primarily the fact that in integrated operation, low-quality steam was used as the heat source, while natural gas with a much higher exergy-to-energy ratio was used in separate operation. These results suggest that integrated operation might be desirable from a thermodynamic efficiency point-of-view as well.

In summary, the previous work on the polygeneration plant suggested that integrated operation was advantageous compared to separate operation for the following reasons:

- Energy cost of the ethanol production might be significantly reduced during integrated operation [26].
- The exergy efficiency of the straw-to-ethanol conversion was markedly higher for integrated operation [27] [15].
- Integrated operation made it possible to run the CHP with lower power production ratios, which could be advantageous in periods of mandatory DH production and low or negative power prices [26].

The present study seeks to quantify the impact of the suggested benefits by optimizing the design and operation of the suggested PGP concept.

3. Design optimization methodology

The pre-synthesized PGP is optimized simultaneously at the design and operation levels with the objective of minimizing the break-even specific ethanol production cost. Furthermore, the yearly average exergy efficiency of the ethanol production is calculated for each solution to the optimization problem in order to evaluate the efficiency of the ethanol production.

3.1. Economic data

Average costs of the energy commodities coal and gas over the reference year 2011, including overhead costs, are summarized in Table 4. Information on the market power price in the Denmark East block for each hour of 2011 was taken from the Nord Pool Spot database [38]. A scatter distribution showing the maximum, minimum, and average daily power prices is shown in Figure 4. The average daily power price ranges from 0.153 Euro/kWh to 0.812 Euro/kWh, while the hourly power price ranges from -0.368 Euro/kWh to 1.902 Euro/kWh. The average yearly power price was 0.494 Euro/kWh.

Costs associated with the production of lignocellulosic ethanol in a full scale facility using IBUS technology, which means a straw processing capacity rate of 1000 tons/day or 11.57 kg/s, were estimated in a feasibility study by Larsen et al. [32]. The values from the feasibility study were used as reference values in the present study and are summarized in Table 5.

3.2. Optimization model description

As far as board decisions and substantial investments are concerned, the main parameter for evaluating a lignocellulosic ethanol production facility is the break-even production cost per liter of

ethanol, c_{eth} [32]. The objective of the optimization problem is to minimize c_{eth} as perceived by the plant owner by varying the design and operation of the plant. The specific ethanol production cost is made up of seven cost components: Specific cost for straw c_{straw}; specific investment depreciation cost c_I; specific operation and maintenance (O&M) costs $c_{O\&M}$; specific cost for enzymes c_{enz}; specific cost for additives c_{add}; specific energy costs c_{energy}; and specific incomes from sales of molasses and solid biofuel c_{sales}.

$$c_{eth} = c_{straw} + c_I + c_{O\&M} + c_{enz} + c_{add} + c_{energy} - c_{sales} \quad (1)$$

3.2.1. Decision variables

At *design level*, the previously found optimal integration design [26] with respect to steam extraction pattern is kept, while the straw processing capacity of the ethanol production σ is varied. The straw processing capacities investigated were set to range from 5 kg/s, being slightly smaller than the capacity of the ethanol production in the reference system, to 12 kg/s, which is about the size of a full scale IBUS ethanol production facility, as reported by Larsen et al. [32]:

$$\sigma \in [5,12] \quad (2)$$

At *operation level*, four decision variables are considered for each operation hour i: The load of the CHP unit λ_i, which can be 0.0 or within the range [0.4; 1.0] [29]; the back-pressure operation parameter α_i, which can be varied within the range 0 to 1, with 0 representing condensation mode operation and 1 representing full back-pressure operation; the relative production of DH in the ethanol facility β_i, which can be varied from 0 to 1; and, finally, a dummy parameter describing the choice between integrated and separate operation κ_i, taking the value 1 for integrated operation and 0 for separate operation.

$$0.40 \leq \lambda_i \leq 1.00 \quad (3)$$

$$0.00 \leq \alpha_i \leq 1.00 \quad (4)$$

$$0.00 \leq \beta_i \leq 1.00 \quad (5)$$

$$\kappa_i \in \{0,1\} \quad (6)$$

No DH production from the ethanol process is considered during separate operation, hence:

$$\beta_i = 0 \ \ | \kappa_i = 0. \quad (7)$$

3.2.2. Constraints

As in the previous studies, the plant is seen as a substitute to AVV1 in the present Danish energy system. As a consequence, two operation constraints were set. Regarding DH production, which is subject to strict legislation, the PGP was set to deliver the same hour-wise amount of heat Q_i over the year as the CHP unit produced in the reference operation, $Q_{i,ref}$:

$$Q_i(\sigma, \lambda_i, \alpha_i, \beta_i, \kappa_i) = Q_{i,ref} \quad \forall\, i \quad (8)$$

With regard to power exports P_i, the plant is allowed to reduce its export in a given hour compared to the reference power export $P_{i,ref}$ as back-up capacity is assumed available in the grid. However, the plant is not allowed to exceed its reference power export in any hour as it is uncertain whether or not there would be buyers for the extra power in the grid at the given price.

$$P_i(\sigma, \lambda_i, \alpha_i, \beta_i, \kappa_i) \leq P_{i,ref} \quad \forall\, i \quad (9)$$

Full hour-wise operation flexibility is assumed for the plant, which means that the choice of parameters in an hour $i + 1$ is independent of the choice of parameters in the preceding hour i.

3.2.3. Model equations

The cost for straw c_{straw} depends on several factors, such as cultivation soil type, crop type, irrigation, farm size, transportation distance, production type (organic or non-organic), etc. [39]. Especially transportation costs are relevant if one considers a plant processing locally distributed biomass. However, as the plant in question is located next to the sea on one side and the city of Copenhagen on the other, straw would most likely have to be imported from other regions, and

transportation costs are therefore assumed to be independent of the processing capacity of the ethanol production. A study by the Danish Energy Agency, Ea Energianalyse, and Wazee [39] estimated that the total cost of straw C_{straw} for energy purposes in Denmark in 2011 was in the range of 48.6-52.5 Euro/ton. To represent the expected higher transportation costs from importing straw from the countryside, the highest straw price of $C_{straw} = 52.5\ Euro/ton$ was used in this study. The specific cost of straw per produced liter of ethanol c_{straw} was calculated according to the following equation:

$$c_{straw} = \frac{\eta_{eth}}{\rho_{eth}} C_{straw} \quad (10)$$

In this equation, η_{eth} is the mass-based conversion efficiency of straw to ethanol in the PGP, as presented in Table 1, while $\rho_{eth} = 785.5 m^3/ton$ is the ethanol density taken from the software Engineering Equation Solver (EES) [33] for a temperature of 15°C and a pressure of 1bar.

The specific depreciation cost for the ethanol production, c_I, is assumed to be derived from a fixed annual depreciation rate, which is directly proportional to the investment cost of the equipment. It is common to apply power laws [40] to calculate the investment cost $I(D)$ of equipment as a function of the equipment dimension D:

$$I(D) = I_0 \left(\frac{D}{D_0}\right)^{M_f} \quad (11)$$

In the equation, I_0 is the investment in a piece of equipment with the base dimension D_0, and M_f is a scaling constant that depends on the type of equipment. Assuming that a capacity power law exists for the entire ethanol facility with a scaling constant M_f, the specific depreciation cost for a facility of capacity σ, $c_I(\sigma)$, is calculated using the following relation:

$$c_I(\sigma) = \left(\frac{\sigma_0}{\sigma}\right) c_{I,0} \left(\frac{\sigma}{\sigma_0}\right)^{M_f} \quad (12)$$

Here, $c_{I,0}$ is the reference depreciation cost presented in Table 5, and $\sigma_0 = 11.57\ kg/s$ is the reference straw processing capacity. In this study, a scaling constant of $M_f = 0.7$ is used, as suggested by Ilic et al. [10] for a similar facility.

Similar to the calculation of the investment, a capacity power law relationship with the same scaling constant M_f is assumed to apply when calculating the specific O&M cost, $c_{O\&M}$:

$$c_{O\&M}(\sigma) = \left(\frac{\sigma_0}{\sigma}\right) c_{O\&M,0} \left(\frac{\sigma}{\sigma_0}\right)^{M_f} \quad (13)$$

In the equation, $c_{O\&M,0}$ is the reference O&M cost associated with a facility of the size σ_0.

The specific energy cost of the ethanol production c_{energy} represents the extra energy costs from operating the PGP compared to the CHP over the reference year, divided by the PGP ethanol production. It consists of three components: Specific cost of extra CHP fuel (coal) c_{fuel}, specific cost of natural gas c_{gas}, and specific cost of power c_{power}:

$$c_{energy} = c_{fuel} + c_{gas} + c_{power} \quad (14)$$

Incomes from DH sales are not associated with the ethanol production as the PGP is set to deliver the same amounts of heat on an hourly basis as the CHP unit in the reference year. Furthermore, costs for external cooling are negligible because of the ready availability of sea water.

The CHP fuel cost for an hour i, $c_{fuel,i}$, is calculated as the difference in fuel cost between the chosen operation and the fuel cost for the reference operation:

$$c_{fuel,i}(\lambda_i) = \frac{\left(Q_{fuel,i}(\lambda_i) - Q_{fuel,i,ref}(\lambda_{i,ref})\right) \cdot c_{coal}}{V_{eth}} \quad (15)$$

Here, $\lambda_{i,ref}$ is the reference CHP unit load, $Q_{fuel,i}(\lambda_i)$ is the actual fuel consumption of the CHP unit, $Q_{fuel,i,ref}(\lambda_{i,ref})$ is the reference fuel consumption of the CHP unit, c_{coal} is the specific coal cost as given in Table 4, and V_{eth} is the hourly ethanol production volume calculated as

$$V_{eth} = \sigma \cdot \frac{\eta_{eth}}{\rho_{eth}} \cdot 3600 s/h \quad (16)$$

Natural gas is consumed only during separate operation. The cost of natural gas in an hour i is a function of the straw processing capacity σ_j and the choice of integrated or separate operation κ_i.

$$c_{NG,i}(\sigma, \kappa_i) = (1 - \kappa_i) \cdot \left[\sigma \left(\frac{q_{steam}+q_{heat}}{\eta_{boiler}}\right) \cdot c_{NG}\right] \qquad (17)$$

Here, $q_{steam} + q_{heat}$ is the total specific heating demand of the ethanol facility, $\eta_{boiler} = 0.96$ is the thermal efficiency of the natural gas boiler and c_{NG} is the specific cost of natural gas, as given in Table 4.

The specific cost of power, c_{power}, represents both the cost of buying power for running the ethanol production during separate operation and the costs of lost power sales in integrated operation when the power exports of the PGP are lower than the reference power exports of the CHP unit. The specific cost of power in an hour i, c_{power}, is calculated as

$$c_{power,i}(\sigma, \lambda_i, \alpha_i, \beta_i, \kappa_i) = \frac{\left[\left(P_{i,ref} - P_i(\sigma,\lambda_i,\alpha_i,\beta_i,\kappa_i)\right) + \kappa_i \cdot P_{eth}(\sigma,)\right] \cdot c_{el,i}}{V_{eth}} \qquad (18)$$

In the equation, $P_{i,ref}$ is reference power production of the CHP unit, P_i is the power production of the PGP, $P_{eth}(\sigma)$ is the power consumption of the ethanol production, and $c_{el,i}$ is the power price in a given hour.

Using equation (14), the specific energy cost in a given hour i, $c_{energy,i}$, is then calculated according to the following equation:

$$c_{energy,i}(\sigma, \lambda_i, \alpha_i, \beta_i, \kappa_i) = \frac{(\lambda_i - \lambda_{i,ref}) \cdot Q_{nom} \cdot c_{coal}}{V_{eth}} + (1 - \kappa_i) \cdot \left[\sigma \left(\frac{q_{steam}+q_{heat}}{\eta_{boiler}}\right) \cdot c_{NG}\right] +$$

$$\frac{[P_{i,ref} - P_i(\sigma,\lambda_i,\alpha_i,\beta_i,\kappa_i)] \cdot c_{el,i}}{V_{eth}} \qquad (19)$$

The yearly average specific energy cost c_{energy} is calculated as

$$c_{energy}(\sigma, \lambda, \alpha, \beta, \kappa) = \frac{\sum_{i=1}^{8760} c_{energy,i}(\sigma,\lambda_i,\alpha_i,\beta_i,\kappa_i)}{8760} \qquad (20)$$

For the specific ethanol production costs, it is assumed that the specific cost for enzymes c_{enz}, additives c_{add}, and the specific incomes from by-product sales c_{sales} are independent of the ethanol facility capacity and operation of the CHP unit. The reference values presented in Table 5 are used for these parameters.

3.2.4. Objective function minimization

Given the equations (1)–(20) for costs and variable constraints, the objective function, which is the break-even specific ethanol production cost, is defined as

$$c_{eth}(\sigma,\lambda,\alpha,\beta,\kappa) = \frac{\eta_{eth}}{\rho_{eth}} C_{straw} + c_{I,0}\left(\frac{\sigma}{\sigma_0}\right)^{M_f} + c_{O\&M,0}\left(\frac{\sigma}{\sigma_0}\right)^{M_f} + c_{enz} + c_{add} - c_{sales} + c_{energy}(\sigma,\lambda,\alpha,\beta,\kappa) \quad (21)$$

The optimization problem can then be formulated as

$$\begin{cases} \min_{\sigma,\lambda,\alpha,\beta,\kappa}[c_{eth}(\sigma,\lambda,\alpha,\beta,\kappa)] \\ \quad subject\ to\ constraints: \\ \text{equations (7), (8)} \\ \quad with\ variables: \\ \sigma_j \in [5,12]; \quad \alpha,\beta \in [0.0,1.0]; \quad \lambda \in [0.4,1.0] \\ \qquad\qquad\qquad \kappa \in \{0,1\} \end{cases} \quad (22)$$

Solving the optimization problem (22) will result in the lowest possible break-even specific ethanol production cost for the treated PGP under the set conditions.

3.2.5. Linearization

As the PGP unit model is non-linear, the optimization problem (22) becomes non-linear. To simplify the calculations, a piece-wise linearization of the model for the integrated PGP operation was introduced. The non-linear operational range of the reference PGP, with a straw processing capacity of $\sigma_{ref} = 6.22$ as described in Section 2, is presented in Figure 5, and six key operational points are indicated. The operational characteristics of the six key operation points are described in Table 6.

The difference in power exports between points (1) and (a) is a direct consequence of the extraction of steam and the consumption of produced power to run the ethanol facility in integrated mode. As the steam extraction and power consumption are both linear functions of the ethanol facility capacity σ, the difference in power yield is assumed to be a linear function of σ as well:

$$\dot{P}_1(\sigma) = \dot{P}_a + \sigma \frac{(\dot{P}_{1,PGP,ref} - \dot{P}_a)}{\sigma_{ref}} = 249.3 - 3.54 \cdot \sigma \quad [MW] \qquad (23)$$

Point (2) relates to point (a) in the sense that the CHP unit is operated in the same way, but with the difference that full ethanol DH production is activated. The maximum DH production from the ethanol facility is a linear function of the straw processing capacity σ, and the reduced power production potential is assumed to be a linear function of σ as well:

$$\dot{Q}_2(\sigma) = \sigma \frac{\dot{Q}_{2,PGP,ref}}{\sigma_{ref}} = 13.07 \cdot \sigma \quad [MJ/s\,] \qquad (24)$$

$$\dot{P}_2(\sigma) = \dot{P}_a + \sigma \frac{(\dot{P}_{2,PGP,ref} - \dot{P}_a)}{\sigma_{ref}} = 249.3 - 3.99 \cdot \sigma \quad [MW] \qquad (25)$$

Point (4) relates to point (c) in a similar way as (2) to (a), while (3) relates to (b) and (6) relates to (d). Using the same approach for these points, the following relations were obtained for heat and power yields in each of the points as a function of σ:

$$\dot{Q}_3(\sigma) = \dot{Q}_b + \sigma \frac{(\dot{Q}_{3,PGP,ref} - \dot{Q}_b)}{\sigma_{ref}} = 332.9 + 1.00 \cdot \sigma \quad [MJ/s\,] \qquad (26)$$

$$\dot{P}_3(\sigma) = \dot{P}_b + \sigma \frac{(\dot{P}_{3,PGP,ref} - \dot{P}_b)}{\sigma_{ref}} = 216.0 - 3.06 \cdot \sigma \quad [MW] \qquad (27)$$

$$\dot{Q}_4(\sigma) = \dot{Q}_c + \sigma \frac{(\dot{Q}_{4,PGP,ref} - \dot{Q}_c)}{\sigma_{ref}} = 163.1 + 2.30 \cdot \sigma \quad [MJ/s\,] \qquad (28)$$

$$\dot{P}_4(\sigma) = \dot{P}_c + \sigma \frac{(\dot{P}_{4,PGP,ref} - \dot{P}_c)}{\sigma_{ref}} = 86.3 - 1.86 \cdot \sigma \quad [MW] \qquad (29)$$

$$\dot{Q}_5(\sigma) = \dot{Q}_c + \sigma \frac{(\dot{Q}_{5,PGP,ref} - \dot{Q}_c)}{\sigma_{ref}} = 163.1 - 8.92 \cdot \sigma \quad [MJ/s\,] \qquad (30)$$

$$\dot{P}_5(\sigma) = \dot{P}_c + \sigma \frac{(\dot{P}_{5,PGP,ref} - \dot{P}_c)}{\sigma_{ref}} = 86.3 - 1.68 \cdot \sigma \quad [MW] \qquad (31)$$

$$\dot{P}_6(\sigma) = \dot{P}_d + \sigma \frac{\left(\dot{P}_{6,PGP,ref} - \dot{P}_d\right)}{\sigma_{ref}} = 104.9 - 2.40 \cdot \sigma \quad [MW] \qquad (32)$$

It is furthermore assumed that for a PGP with straw processing capacity σ, the maximum and minimum potential power productions in integrated operation, $\dot{P}_{max}$ and $\dot{P}_{min}$, are piece-wise linear functions of the heat production $\dot{Q}$ between the key operation points according to the following relations:

$$\dot{P}_{max}(\dot{Q}, \sigma) = \begin{cases} \dot{P}_1(\sigma) + \dot{Q}\left(\frac{\dot{P}_2(\sigma) - \dot{P}_1(\sigma)}{\dot{Q}_2(\sigma) - \dot{Q}_1(\sigma)}\right) & | \ \dot{Q} \in \left[\dot{Q}_1(\sigma), \dot{Q}_2(\sigma)\right] \\ \dot{P}_2(\sigma) + \left(\dot{Q} - \dot{Q}_2(\sigma)\right)\left(\frac{\dot{P}_3(\sigma) - \dot{P}_2(\sigma)}{\dot{Q}_3(\sigma) - \dot{Q}_2(\sigma)}\right) & | \ \dot{Q} \in \left]\dot{Q}_2(\sigma), \dot{Q}_3(\sigma)\right] \end{cases} \qquad (33)$$

$$\dot{P}_{min}(\dot{Q}, \sigma) = \begin{cases} \dot{P}_6(\sigma) + \dot{Q}\left(\frac{\dot{P}_5(\sigma) - \dot{P}_6(\sigma)}{\dot{Q}_5(\sigma) - \dot{Q}_6(\sigma)}\right) & | \ \dot{Q} \in \left[\dot{Q}_6(\sigma), \dot{Q}_5(\sigma)\right] \\ \dot{P}_5(\sigma) + \left(\dot{Q} - \dot{Q}_5(\sigma)\right)\left(\frac{\dot{P}_4(\sigma) - \dot{P}_5(\sigma)}{\dot{Q}_4(\sigma) - \dot{Q}_5(\sigma)}\right) & | \ \dot{Q} \in \left]\dot{Q}_5(\sigma), \dot{Q}_4(\sigma)\right] \\ \dot{P}_4(\sigma) + \left(\dot{Q} - \dot{Q}_4(\sigma)\right)\left(\frac{\dot{P}_3(\sigma) - \dot{P}_4(\sigma)}{\dot{Q}_3(\sigma) - \dot{Q}_4(\sigma)}\right) & | \ \dot{Q} \in \left]\dot{Q}_4(\sigma), \dot{Q}_3(\sigma)\right] \end{cases} \qquad (34)$$

Evaluating the piece-wise linearized model (23)-(34) for the PGP with the reference straw processing capacity, the deviation of the power values between the key operation points was found to be in the range of -0.69% to +0.77% when compared to the non-linear thermodynamic model.

The load λ of the CHP unit on the line between the points (3) and (4) in Figure 5 is seen as a linear function of the heat production $\dot{Q}$ as well:

$$\lambda(\dot{Q}) = \lambda_3 + \left(\dot{Q} - \dot{Q}_3(\sigma)\right)\frac{(\lambda_4 - \lambda_3)}{\left(\dot{Q}_4(\sigma) - \dot{Q}_3(\sigma)\right)} = 1 - 0.6\frac{\left(\dot{Q} - \dot{Q}_3(\sigma)\right)}{\left(\dot{Q}_4(\sigma) - \dot{Q}_3(\sigma)\right)} \quad |\dot{Q} \in \left[\dot{Q}_4(\sigma), \dot{Q}_3(\sigma)\right] \qquad (35)$$

The linearization (35) was found to have an accuracy of -0.00% to 3.0% as compared to the non-linear thermodynamic model.

Finally, the fuel consumption of the CHP unit as a function of the load λ, $Q_{fuel}(\lambda)$, was linearized using the linear trendline-function in Microsoft Excel:

$$Q_{fuel,i}(\lambda_i) = 1798.7 \cdot \lambda_i + 367.8 \ [GJ/h] \qquad (36)$$

The coefficient of determination for the approximated equation (36) was found to be 0.9998 when compared to the fuel consumption predicted in the thermodynamic model of the CHP unit.

Applying (23)-(36) and taking the optimization constraints into account, the optimal operation solution space is reduced *a priori* to the following four operation points for each hour.

1) Integrated operation with maximum power delivery
2) Integrated operation with minimum power delivery
3) Separate operation with maximum power delivery
4) Separate operation with zero CHP load

The reasoning is that under the given assumptions, separate operation is advantageous only when the cost of lost power sales is higher than the cost of natural gas for running the ethanol production. However, for the 2060 hours during which the CHP unit was shut down in the reference scenario, the PGP is forced to operate in separate mode as well. When integrated operation is advantageous, it is either optimal to maximize or minimize power production, depending on whether income from power sales is higher or lower than the cost for CHP fuel.

3.3. Thermodynamic performance evaluation

The thermodynamic performance of any design solution is evaluated by calculating the average yearly exergy efficiency η_{ex} of the ethanol production:

$$\eta_{ex} = \frac{\sum_{i=1}^{8760} \eta_{ex,i}}{8760} \quad (37)$$

In eq. (37), $\eta_{ex,i}$ is the hour-wise exergy efficiency of the ethanol production. Using the exergy analysis method described in Lythcke-Jørgensen et al. [15] for calculating exergy contents of the flows in the ethanol production, the hourly exergy efficiency is calculated as

$$\eta_{ex,i} = \frac{\sum \dot{EX}_{products,i}}{\sum \dot{EX}_{in,i}} \quad (38)$$

Here $\sum \dot{EX}_{in,i}$ is the sum of exergy contents in the power and natural gas or steam into the system over the hour i. $\sum \dot{EX}_{products,i}$ is the sum of exergy contents in the products delivered over the hour i, be it ethanol, molasses, solid biofuel, or, potentially, district heating. The calculated exergy contents of biomass flows per kg of biomass treated and the exergy content of the natural gas flow during integrated and separate operation are presented in Table 7.

The exergy content of the steam extracted from the CHP unit during integrated operation depends on the chosen operation mode according to the decision variables $\{\lambda_i, \alpha_i, \beta_i, \kappa_i\}$. The exergy content of the extracted steam in a given hour $\dot{EX}_{steam,i}$ was calculated directly in the PGP model, and the corresponding specific exergy content per kg of straw treated $ex_{steam,i}$ was calculated using the following equation:

$$ex_{steam,i}(\lambda_i, \alpha_i, \beta_i, \kappa_i) = \frac{\dot{EX}_{steam,i}(\lambda_i, \alpha_i, \beta_i, \kappa_i)}{\sigma} \qquad (39)$$

4. Results

4.1. Cost minimization

When solving the optimization problem (22), the specific ethanol production cost obtained is plotted as a function of σ in Figure 6 together with four of the key specific cost components: Specific energy costs, specific straw cost, specific O&M costs, and specific investment depreciation cost. The lowest specific ethanol production cost, $c_{eth} = 0.958\ Euro/L$, was obtained for $\sigma = 5kg/s$. The specific energy cost, on an average 0.517 Euro/L over the year for this solution, was found to be the largest single post in the total specific ethanol production cost. Average specific energy costs were found to be 0.213 Euro/L during integrated operation and 1.192 Euro/L during separate operation for the optimal solution, underlining the economic inefficiency of the separate operation. Comparing these costs to an average ethanol price of 0.55 Euro/L on the European

478 market in the period 2008-2010 [41], the results suggest that even the optimal design is
479 uncompetitive, mainly due to the duration of separate operation.
480 An important outcome of the study is the diseconomies-of-scale trend that is found to apply for the
481 ethanol production costs, which is in contrast to the commonly accepted economies-of-scale
482 principle. In the present case, the diseconomy-of-scale is directly related to the energy costs of the
483 production whose increase with increased capacity σ exceeds the capacity-dependent decrease in
484 specific investment costs and O&M costs, as shown in Figure 6.
485 The increase in specific energy costs with σ was found to be a consequence of changes in the
486 operation pattern. Figure 7 shows the optimal operation characteristics of the solutions as a function
487 of σ, and it is seen that the duration of separate operation increases with increased σ. This effect was
488 caused by high power prices and the reduced power production potential during integrated
489 operation with increasing σ, causing the cost of lost power sales to exceed the cost of running the
490 PGP in separate operation for an increasing amount of hours over the year.
491 In Figure 8, this effect is further highlighted by plotting the components of the specific energy cost
492 as a function of σ. It is seen that the specific costs for power and gas increased with increasing σ
493 because of the longer duration of separate operation, causing the overall specific energy costs to
494 increase. The specific coal cost is seen to decrease with increased σ owing to the decreased duration
495 of integrated operation.
496 Another significant outcome with respect to operation is the low duration of integrated operation in
497 minimum load. As described in Section 2.2, one of the three assumed advantages of the integrated
498 system was the potential of reducing power production in periods with low or negative power prices.
499 However, in the East Denmark power block anno 2011, the solution to the optimization problem
500 (22) found it optimal to use this advantage for only 104h over the year. For the rest of the integrated
501 operation points, the economical optimization maximized the power production within the set

operational constraint (9). This is further evident from the scatter distribution of the optimal quasi-static hourly operation points for the solution with $\sigma = 5kg/s$ shown in Figure 9, where only a few of the optimal operation points are found on the lower boarder of the feasible operation range. The main reason for the short use of this advantage is the low coal price and the resultant low break-even electricity production cost in the CHP unit, making it economically unattractive to minimize power production unless power prices are very low. What is further worth noticing in Figure 9 is the gap between the upper boarder of the feasible operation range for integrated operation and the separate operation points. For the reference operation points located in this gap, the optimization found that the costs for sustaining integrated operation in terms of lost power sales were lower than the corresponding energy costs for running separate operation, hence integrated operation was preferred.

4.2. Thermodynamic performance

The exergy efficiency for the ethanol production in each of the operation points over the year was calculated. Results for selected operation points are presented in Table 8.

It is seen that the exergy efficiency of the ethanol production is significantly higher for integrated operation than for separate operation, mainly owing to the fact that steam from the CHP unit is replaced by natural gas, with a very high exergy-to-energy ratio, as the hot utility source during separate operation. Furthermore, the results suggest that the exergy efficiency is higher when full district heating production is activated in the ethanol facility because the exergy content of the waste heat from the processes, which would otherwise be lost to external cooling, is contained in the product 'district heating'. Finally, the exergy efficiency was found to increase with reduced load λ_i in the intervals 0.4-0.6 and 0.6-1.0. The reason for the increased efficiencies with reduced λ_i is the fact that the exergy content of the extracted steam decreases with decreased λ_i, as indicated by the values in Table 3. At loads below 0.6, the steam is extracted in a different pattern than for loads

526 of 0.6 or higher in the CHP unit, as explained in Section 2, causing the break in the exergy
527 efficiency trend at this point.
528 The yearly average exergy efficiency of the ethanol production for the optimal operation pattern as
529 a function of σ is plotted in Figure 10. The average exergy efficiency is found to decrease with
530 increased σ, mainly owing to the increased duration of separate operation. The highest yearly
531 average exergy efficiency of $\eta_{II} = 0.746$ was obtained for the optimal operation pattern for
532 $\sigma = 5kg/s$.
533 A Grassmann diagram illustrating the yearly average exergy flows in the ethanol production for the
534 optimal solution, $\sigma = 5kg/s$ is presented in Figure 11. It is seen that the main part of exergy losses
535 and destruction (L&D) occurs in the heat integration network, which is mainly caused by two
536 factors: The use of high-quality natural gas as heat source in separate operation and the fact that
537 waste heat is not always used for DH production.
538 Evaluating the simulation results for the optimized solutions, another interesting outcome was
539 found with respect to thermodynamic performance of the PGP: The increase in CHP coal
540 consumption in MJ/s during integrated operation was lower than the energy in the extracted steam
541 in MJ/s to run the ethanol production when DH production was activated in the ethanol facility. The
542 cause of this phenomenon was the DH production from waste heat in the ethanol facility: It allowed
543 the CHP unit to reduce the steam extraction from turbines for DH production without
544 compromising the total DH production, thereby allowing higher levels of power production in the
545 CHP unit. A similar phenomenon was described for an analogue system by Starfelt et al. [17]. This
546 suggests that not just the exergy efficiency, but also the overall energy efficiency is higher for the
547 integrated production of lignocellulosic ethanol.

4.3. Sensitivity analysis

As several of the cost values are based on assumptions or approximations, a sensitivity analysis was carried out for nine parameters in the optimal solution in order to investigate the impact on the production cost of the break-even specific ethanol production cost. The results are presented in a spider plot in Figure 12.

It is seen that variations in straw price, natural gas price, and the value of the sold by-products will have the highest impact on the specific ethanol production price. On the other hand, it is also seen that the break-even specific ethanol production cost is hardly affected by variations in coal price. What is further of interest is the fact that an increase in the power law scaling constant will reduce the specific ethanol production cost because the capacity of the optimal solution is smaller than the reference capacity; a higher capacity power factor will therefore limit the increases in specific costs for O&M and depreciation for the smaller facility.

Although having the highest impact on specific ethanol production costs, the straw price does not affect the optimal dimension of the ethanol facility, as it is kept constant. Furthermore, as seen in Figure 6, O&M, investment and depreciation costs were less significant than specific energy costs when determining the optimal dimension. As historical data were used for power price and heat demand, it was investigated if changes in the assumed coal and natural gas prices would affect the optimal dimension. However, varying the value of each of the parameters from 0% to 1000% of the assumed value, the optimal design remained unchanged. This suggests that the diseconomy-of-scale trend identified prevails even in case of major changes in fuel costs occurred.

5. Discussion

For the PGP treated in this study, integrated operation was found to be advantageous when compared to separate operation as it achieved a lower specific energy cost, a higher first law energy

efficiency for the entire PGP, when district heating production was activated in the ethanol facility, and a higher ethanol production exergy efficiency. These outcomes all comply with results reported by other studies on integrating lignocellulosic ethanol in CHP units. As a consequence, the expected long duration of separate operation over the year even for the optimal solution poses a major challenge for the ambition of reducing the costs of lignocellulosic ethanol production by integrating it with the CHP plant. The duration of separate operation over the year was found to increase with increased straw processing capacity σ of the ethanol facility, resulting in a diseconomy-of-scale trend for the suggested integration scheme. This trend was caused by the reduced power production potential with increased σ for integrated PGP operation, often making the cost of lost power sales exceed the costs of the inefficient separate operation.

For the optimal solution, separate operation occurred for 2718h over the year, of which the 2060h were caused by CHP unit down-time. The simplest way to increase the duration of integrated operation would be to reduce the duration of CHP unit down-time. Whether this is feasible for the given CHP unit is uncertain, but in general it underlines the importance of considering integration availability when integrating biomass-conversion processes in CHP units, a topic also discussed by Kohl et al. [42]. It should be mentioned here that the choice of reference year has a significant impact on the outcomes, as abnormalities in the chosen reference year affect the overall evaluation results. Whether or not 2011 is suitable as a reference year for the suggested polygeneration scheme should be investigated further before any final conclusion can be drawn with respect to the competitiveness of the suggested scheme. For instance, Starfelt et al. [18] considered a down-time of only 326h for a CHP unit in their study, which however was the sole producer of heat in a local district heating network. Opposed to this, AVV1 competes with other heat producers in the greater Copenhagen district heating network, so the prolonged down-time could be a result of economic decisions. If so, the decisions may have been altered if ethanol production had been integrated in the

595 CHP unit, which would have provided different options for optimizing operation economy in
596 otherwise unfavourable market conditions, e.g. by minimizing power production while sustaining
597 integrated mode operation.
598 When conducting the optimization on design and operation levels, it was assumed that the ethanol
599 production was to be sustained at full load all year round. However, it might be possible to reduce
600 the duration of separate operation if the load could be varied in the ethanol production, or if the
601 straw pretreatment could be performed in batches. This would allow integrated operation during
602 periods of lower power demands and no pretreatment during periods of high power demands,
603 thereby significantly increasing the power production potential in integrated operation.
604 Furthermore, the energy demands of the separation stage could possibly be reduced by applying
605 state-of-the-art mechanical separation technologies. It is, however, beyond the scope of the present
606 paper to evaluate whether or not these suggestions are technologically feasible.
607 Another assumption during the optimization was the constraint that the PGP had to meet the heat
608 production of the reference CHP unit for each hour of the year. If sufficient heat storage capacity
609 was available, it might be possible to relax this constraint by assuming that the total production over
610 a period of 24h had to be met instead of the hour-wise production. This would allow operation
611 flexibility within the 24h periods and, potentially, longer durations of integrated operation over the
612 year as well.
613 A simplification of the calculations entailed the assumption of constant biomass price independently
614 of the processing capacity of the ethanol production. However, this assumption may not be valid for
615 at least two reasons: Firstly, transportation costs will most likely increase with increased biomass
616 consumption due to the distributed nature of straw, the biomass processed in this system [43]. And
617 secondly, large-scale consumption of straw would induce competition with other straw-consumers
618 causing straw prices to increase further. Such developments in the straw price might increase the

619 diseconomies-of-scale trend for the costs of the integrated ethanol production. A more robust straw
620 cost calculation model, taking into account the straw supply chain and competing uses, is a topic of
621 future research for the authors.
622 One of the benefits of the suggested PGP is its ability to reduce the power production without
623 compromising heat production during periods of low or negative power prices. For the optimal
624 solution, this advantage was exploited for 104h over the year of 2011. In the future, this advantage
625 may become more pronounced as an increased production from intermittent renewable energy
626 sources is integrated in the energy system, increasing the demand for balancing means in the heat-
627 and-power sectors [1] and potentially providing another *raison d'être* for the PGP. However, in
628 order to predict the development of the energy system, advanced energy system analysis methods
629 [44] should preferably be applied. Integration of energy system analysis with the synthesis, design,
630 and operation optimization of PGPs is another topic for future research for the authors.
631 Concludingly, the results of the study point towards two overall outcomes: Firstly, they question the
632 efficiency of integrating lignocellulosic ethanol production in the Danish CHP unit AVV1 in the
633 present energy system. Secondly, they illustrate how operating conditions may have a significant
634 impact on plant performance; for the PGP in question, design point operation predicted a specific
635 energy cost of 0.213 Euro/L ethanol produced and an exergy efficiency in the range 0.842-0.855,
636 while a performance optimization with respect to expected operating conditions yielded a best-case
637 average specific energy cost of 0.517 Euro/L ethanol and a yearly average exergy efficiency of
638 0.746.

639 ## 6. Conclusion

640 This study treats the simultaneous optimization of design and operation levels for a polygeneration
641 plant in which hydrothermal pretreatment-based lignocellulosic ethanol production is assumed

integrated in the Danish combined heat and power unit Avedøreværket 1. The objective of the optimization is to minimize the specific ethanol production costs, as perceived by the plant owner. The optimization considers straw processing capacities in the ethanol production ranging from 5 kg/s to 12 kg/s, and quasi-static hour-wise operation over a year. The polygeneration plant operation is constrained by a fixed hourly heat production and an upper limit for the hourly power exports. Capacity power laws are used for predicting specific costs of investment depreciation and operation and maintenance (O&M), while the energy cost is calculated as a function of the operation over the year.

The results suggests that diseconomies of scale applies to specific ethanol production costs in the integrated polygeneration plant, with the lowest feasible specific ethanol production cost of 0.958 Euro/L being obtained for the design with the smallest ethanol facility capacity considered. The cause of the diseconomies-of-scale phenomenon is the high reference power production of the CHP unit, causing the costs from lost power sales and separate operation to exceed the economies-of-scale benefits from investment depreciation and O&M when increasing ethanol production capacity. A thermodynamic performance evaluation further indicate that the design with the smallest ethanol production capacity is optimal in terms of average yearly exergy efficiency of the ethanol production as well, as it obtains the shortest duration of exergy-wise less efficient separate operation over the year. A sensitivity analysis indicates that variations in straw price and by-products value would have the most significant impact on the specific ethanol production costs, whereas the optimum is indifferent to major variations in fossil fuel prices.

In summary, the outcomes of this study question the economic viability and thermodynamic efficiency of integrating lignocellulosic ethanol production in a combined heat and power unit under the given conditions. Furthermore, the outcomes point towards the importance of considering operating conditions when developing flexible polygeneration plant concepts.

Acknowledgements

The authors would like to acknowledge DONG Energy for their financial support of the research, and Brian Elmegaard for allowing the use of his numerical model of the Danish combined heat and power unit Avedøreværket 1 in the study.

References

[1] H. Lund, Renewable energy systems: the choice and modelling of 100% renewable solutions, Burlington, USA: Elsevier, 2010.

[2] O. Edenhofer, R. Pichs-Madruga and Y. Sokona, "Renewable Energy Sources and Climate Change Mitigation," Intergovernmental Panel on Climate Change and Cambridge University Press, New York, USA, 2012.

[3] J. P. W. Scharlemann and W. F. Laruance, "How green are biofuels?," *Environmental Science,* no. 319, pp. 43-44, 2008.

[4] M. Gassner and F. Maréchal, “Increasing Efficiency of Fuel Ethanol Production from Lignocellulosic Biomass by Process Integration,” *Energy Fuels,* no. 27, pp. 2107-2115, 2013.

[5] M. Balat, "Production of bioethanol from materials via the biochemical pathway: A review," *Energy Conversion and Management,* no. 52, pp. 858-875, 2010.

[6] US Environmental Protection Agency, Green Chemistry Programme, "Basic Information," 8 August 2012. [Online]. Available: http://www.epa.gov/greenchemistry/pubs/basic_info.html. [Accessed 5 August 2013].

[7] S. Lee and Y. T. Shah, “Ethanol from Lignocellulose,” in *Biofuels and Bioenergy: Processes and Technologies,* Boca Raton, Florida, USA, Taylor & Francis Group, 2013, pp. 93-146.

[8] M. Gassner and F. Maréchal, "Thermo-economic optimisation of the polygeneration of synthetic natural gas (SNG), power and heat from lignocellulosic biomass by gasification and methanation," *Energy & Environmental Science*, no. 5, pp. 5768-5789, 2012.

[9] L. Daianova, E. Dotzauer, E. Thorin and J. Yan, "Evaluation of a regional bioenergy system with local production of biofuel for transportation, integrated with a CHP plant," *Applied Energy*, no. 92, pp. 739-749, 2011.

[10] D. D. Ilic, E. Dotzauer and L. Trygg, "District heating and ethanol production through polygeneration in Stockholm," *Applied Energy*, no. 91, pp. 214-221, 2011.

[11] P. Bösch, A. Modarresi and A. Friedl, "Comparison of combined ethanol and biogas polygeneration facilities using exergy analysis," *Applied Thermal Engineering*, no. 37, pp. 19-29, 2012.

[12] A. Modarresi, P. Kravanja and A. Friedl, "Pinch and exergy analysis of lignocellulosic ethanol, biomethane, heat and power production from straw," *Applied Thermal Engineering*, no. 43, pp. 20-28, 2012.

[13] S. Leduc, F. Starfelt, E. Dotzauer, G. Kindermann, I. McCallum, M. Obersteiner and J. Lundgren, "Optimal location of lignocellulosic ethanol refineries with polygeneration in Sweden," *Energy*, no. 35, pp. 2709-2716, 2010.

[14] R. Palacios-Bereche, K. J. Mosqueira-Salazar, M. Modesto, A. V. Ensinas, S. A. Nebra, L. M. Serra and M.-A. Lozano, "Exergetic analysis of the integrated first- and second-generation ethanol production from sugarcane," *Energy*, no. 62, pp. 46-61, 2013.

[15] C. Lythcke-Jørgensen, F. Haglind and L. R. Clausen, "Exergy analysis of a combined heat and power plant with integrated lignocellulosic ethanol production," *Energy Conversion and Management*, vol. 85, no. 817-827, 2014.

[16] N. S. Bentsen, B. j. Thorsen and C. Felby, "Energy, feed and land-use balances of refining winter wheat to ethanol," *Biofuels, Bioproducts & Biorefining,* no. 3, pp. 521-533, 2009.

[17] F. Starfelt, E. Thorin, E. Dotzauer and J. Yan, "Performance evaluation of adding ethanol production into an existing combined heat and power plant," *Bioresource Technology,* no. 101, pp. 613-618, 2009.

[18] F. Starfelt, L. Daianova, J. Yan, E. Thorin and E. Dotzauer, "The impact of lignocellulosic ethanol yields in polygeneration with district heating – A case study," *Applied Energy,* no. 92, pp. 791-799, 2012.

[19] C. A. Frangopoulos, M. R. von Spakovsky and E. Scubba, "A Brief Review of Methods for the Design and Synthesis Optimization of Energy Systems," *International Journal of Applied Thermodynamics,* no. 4, pp. 151-160, 2002.

[20] P. Voll, M. Lampe, G. Wrobel and A. Bardow, "Superstructure-free synthesis and optimization of distributed industrial energy supply systems," *Energy,* no. 45, pp. 424-435, 2012.

[21] H. Lund, A. N. Andersen, P. A. Østergaard, B. V. Mathiesen and D. Connolly, "From electricity smart grids to smart energy systems - A market operation based approach and understanding," *Energy,* no. 42, pp. 96-102, 2012.

[22] Y. Chen, T. A. Adams II and P. I. Barton, "Optimal Design and Operation of Flexible Energy Polygeneration Systems," *Industrial & Engineering Chemistry Research,* no. 50, pp. 4553-4566, 2011.

[23] C. Rubio-Maya, J. Uche and A. Martínez, "Sequential optimization of a polygeneration plant," *Energy Conversion and Management,* no. 52, pp. 2861-2869, 2011.

[24] E. F. Grisi, J. M. Yusta and H. M. Khodr, "A short-term scheduling for the optimal operation of biorefineries," *Energy Conversion and Management,* no. 52, pp. 447-456, 2011.

[25] J. Larsen, M. Østergaard Haven and L. Thirup, “Inbicon makes lignocellulosic ethanol a commercial reality,” *Biomass and Bioenergy,* no. 46, pp. 36-45, 2012.

[26] C. Lythcke-Jørgensen, F. Haglind and L. R. Clausen, "Thermodynamic and economic analysis of integrating lignocellulosic bioethanol production in a Danish combined heat and power plant," in *21st European Biomass Conference & Exhibition*, Copenhagen, Denmark, 2013, June 3-7.

[27] C. Lythcke-Jørgensen, F. Haglind and L. R. Clausen, "Exergy analysis of a combined heat and power plant with integrated lignocellulosic ethanol production," in *International Conference on Efficiency, Cost, Optimization, Simulation, and Environmental Impact of Energy Systems*, Guilin, China, 2013, July 16-19.

[28] A. Bejan, G. Tsatsaronis and M. Moran, Thermal Design & Optimization, John Wiley & Sons, Inc., 1996.

[29] B. Elmegaard and N. Houbak, “Simulation of the Avedøreværket Unit 1 cogeneration plant with DNA,” in *16th International Conference on Efficiency, Cost, Optimization, Simulation and Environmental Impact of Energy Systems*, Kgs. Lyngby, Denmark, 2003, June 30 - July 2.

[30] H. Spliethoff, Power Generation from Solid Fuels, München, Germany: Springer-Verlag Berlin Heidelberg, 2010.

[31] B. Elmegaard and N. Houbak, "DNA - A General Energy System Simulation Tool," in *SIMS 2005 : 46th Conference on Simulation and Modeling, pp. 43-52*, Trondheim, Norway, 2005, October 13-14.

[32] J. Larsen, M. Ø. Petersen, L. Thirup, H. W. Li and F. K. Iversen, “The IBUS Process - Lignocellulosic Bioethanol Close to a Commercial Reality,” *Chemical Engineering & Technology,* no. 5, pp. 765-772, 2008.

[33] "F-Chart Software," [Online]. Available: http://www.fchart.com/ees/. [Accessed 25 February 2013].

[34] M. Østergaard Petersen, J. Larsen and M. Hedegaard Thomsen, "Optimization of hydrothermal pretreatment of wheat straw for production of bioethanol at low water consumption without addition of chemicals," *Biomass and Bioenergy,* no. 33, pp. 834-840, 2009.

[35] Energistyrelsen, "Technology Data for Energy Plants," Danish Energy Agency, 2010.

[36] I. C. Kemp, Pinch Analysis and Process Integration, 2nd edition, Oxford, UK: Butterworth-Heinemann, 2006.

[37] N. S. Bentsen, C. Felby and K. H. Ipsen, "Energy Balance of 2nd Generation Bioethanol Production in Denmark," Elsam A/S, 2006.

[38] NordPoolSpot, "Nord Pool Spot," 2011. [Online]. Available: http://www.nordpoolspot.com/. [Accessed 22 June 2012].

[39] Ea Energianalyse, Energistyrelsen, Wazee, "Opdatering af samfundsøkonomiske brændselspriser," Ea Energianalyse, Copenhagen, Denmark, 2011.

[40] R. Smith, Chemical Process Design and Integration, West Sussex, England: John Wiley & Sons Ltd, 2005.

[41] Statens Energimyndighet, "Energiläget 2011," Statens Energimyndighet, Eskilstuna, Sweden, 2011.

[42] T. Kohl, T. Laukkanen, M. Järvinen and C.-J. Fogelholm, "Energetic and environmental performance of three biomass upgrading processes integrated with a CHP plant," *Applied Energy,* no. 107, pp. 124-134, 2013.

[43] M. W. Jack, "Scaling laws and technology development strategies for biorefineries and

bioenergy plants.," *Bioresource Technology,* no. 100, pp. 6324-6330, 2009.

[44] D. Connolly, H. Lund, B. Mathiesen and M. Leahy, "A review of computer tools for analysing the integration of renewable energy in various energy systems," *Applied Energy,* no. 87, pp. 1059-1082, 2010.

672

673

Table 1

Table 1 – Mass conversion efficiencies of the products in the modelled ethanol facility.

Mass conversion efficiency	Nomenclature	Value [-]
Ethanol	η_{eth}	0.150
Molasses	η_{mol}	0.371
Solid biofuel	$\eta_{biofuel}$	0.407

Table 2

Table 2 – Specific energy utility requirements of the ethanol production for operation with zero and full DH production in the ethanol facility.

Utility	Nomenclature	Energy [MJ/kg] - zero DH	Energy [MJ/kg] - full DH	Temperature [°C]	Pressure [bar]
Steam	q_{steam}	5.5	5.5	195	13
Heating	q_{heat}	5.7	8.0	>100	-
Cooling	q_{cool}	11.5	1.0	<20	-
Power	p	0.792[a]	0.792[a]	-	-

[a] A constant power consumption of 220 kWh/ton of straw treated was used as suggested by Bentsen et al. [32].

Table 3

Table 3 – Temperature (T), pressure (P), and specific exergy content (ex) of steam in the extraction points (A), (B), and (C) at various loads.

CHP Load	(A)			(B)			(C)		
	T [C]	P [bar]	ex [kJ/kg]	T [C]	P [bar]	ex [kJ/kg]	T [C]	P [bar]	ex [kJ/kg]
1.0	467	34.2	1274	393	20.5	1121	289	9.2	911
0.9	449	31.1	1240	376	18.6	1090	275	8.3	885
0.8	431	27.9	1204	359	16.7	1058	261	7.5	858
0.7	431	25.1	1192	360	15.0	1046	262	6.7	846
0.6	432	22.1	1179	361	13.2	1032	263	6.0	832
0.5	432	18.9	1161	361	11.3	1014	264	5.1	814
0.4	433	15.5	1138	362	9.3	991	266	4.2	791

Table 4

Table 4 – Energy commodity costs used in the calculations.

Energy commodity	Nomenclature	Specific cost
Coal (CHP fuel)	c_{coal}	4.36 Euro/GJ [33]
Natural gas	c_{NG}	9.26 Euro/GJ [33]

Table 5

Table 5 – Production costs per litre of lignocellulosic ethanol produced in a full scale ethanol facility based on IBUS technology. Values from Larsen et al. [27].

Cost parameter	Nomenclature	Specific cost
Enzymes cost	$c_{enz,0}$	0.14 Euro/L
Additives cost	$c_{add,0}$	0.06 Euro/L
Operation and maintenance cost	$c_{O\&M,0}$	0.09 Euro/L
Depreciation cost	$c_{I,0}$	0.07 Euro/L
By-product sales (molasses and solid biofuel)	$c_{sales,0}$	0.24 Euro/L

Table 6

Table 6 – Operation characteristics and reference production values for the key operation points shown in Figure 5.

Point	CHP unit load, λ [-]	Back-pressure operation parameter, α [-]	Ethanol facility heat production, β [-]	Reference PGP power production, $\dot{P}_{ref}$ [MW]	Reference PGP DH production, $\dot{Q}_{ref}$ [MJ/s]
(1)	1.0	0.0	0.0	227.2	0.0
(2)	1.0	0.0	1.0	224.5	81.3
(3)	1.0	1.0	1.0	197.0	339.1
(4)	0.4	1.0	1.0	74.8	177.4
(5)	0.4	1.0	0.0	75.9	111.5
(6)	0.4	0.0	0.0	89.9	0.0
(a)	1.0	0.0	-	249.3	0.0
(b)	1.0	1.0	-	216.0	332.9
(c)	0.4	1.0	-	86.3	163.1
(d)	0.4	0.0	-	104.9	0.0

Table 7

Table 7 – Exergy content of biomass flows in the ethanol production per kg of straw treated. Values from Lythcke-Jørgensen et al. [22].

Flow description	Exergy content [MJ] – integrated operation	Exergy content [MJ] – separate operation
Straw	16.4	16.4
Natural gas	0.0	12.2
Steam	3.7 – 4.7 [a]	0
Fermentation broth	10.9	10.9
Liquid fraction from pretreatment	5.9	5.9
Ethanol	4.2	4.2
Molasses	4.4	4.4
Solid biofuel	8.0	8.0

[a] The energy consumption for the ethanol production increases with increased DH production, while the specific exergy content of extracted steam depends on operation mode of the CHP unit.

Table 8

Table 8 – Exergy efficiency of the ethanol production in various operating points.

CHP Load, λ_i	Exergy efficiency, η_{II}	
	$\alpha_i = 0, \quad \beta_i = 0$	$\alpha_i = 1, \quad \beta_i = 1$
1.0	0.786	0.842
0.9	0.789	0.845
0.8	0.791	0.849
0.7	0.793	0.851
0.6	0.796	0.854
0.5	0.791	0.850
0.4	0.795	0.855
Separate operation	0.564	

Figure 1

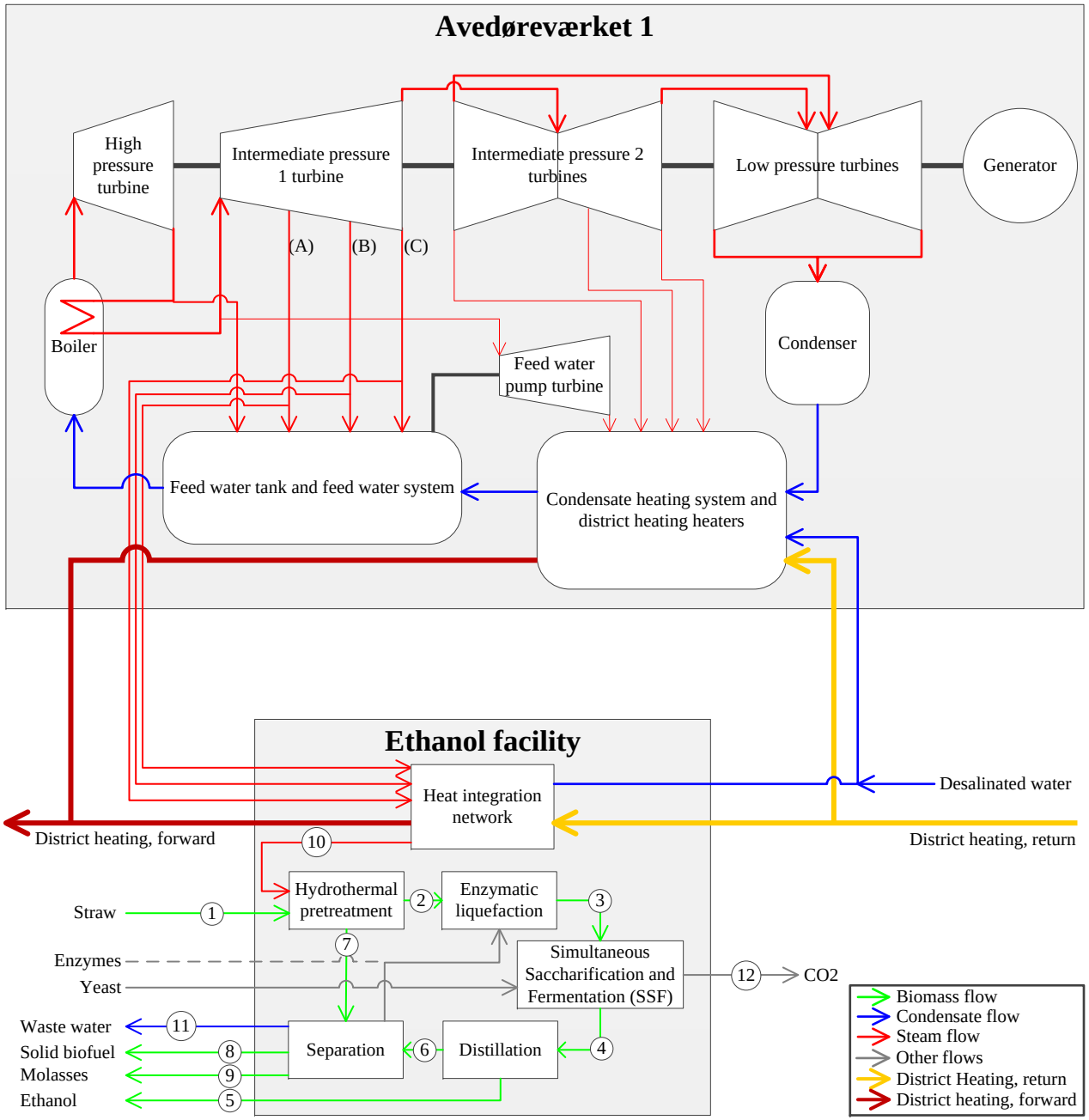
Avedøreværket 1
High pressure turbine
Intermediate pressure 1 turbine
Intermediate pressure 2 turbines
Low pressure turbines
Generator
(A)
(B)
(C)
Boiler
Feed water pump turbine
Condenser
Feed water tank and feed water system
Condensate heating system and district heating heaters
Ethanol facility
Heat integration network
Desalinated water
District heating, forward
District heating, return
10
Hydrothermal pretreatment
2
Enzymatic liquefaction
3
Straw
1
7
Enzymes
Yeast
Simultaneous Saccharification and Fermentation (SSF)
12
CO2
Waste water
11
Solid biofuel
8
Molasses
9
Ethanol
5
Separation
6
Distillation
4
Biomass flow
Condensate flow
Steam flow
Other flows
District Heating, return
District heating, forward

Figure 1 - caption

Figure 1 – Simplified process layout of the polygeneration plant in question. From Lythcke-Jørgensen et al. [22].

Figure 2

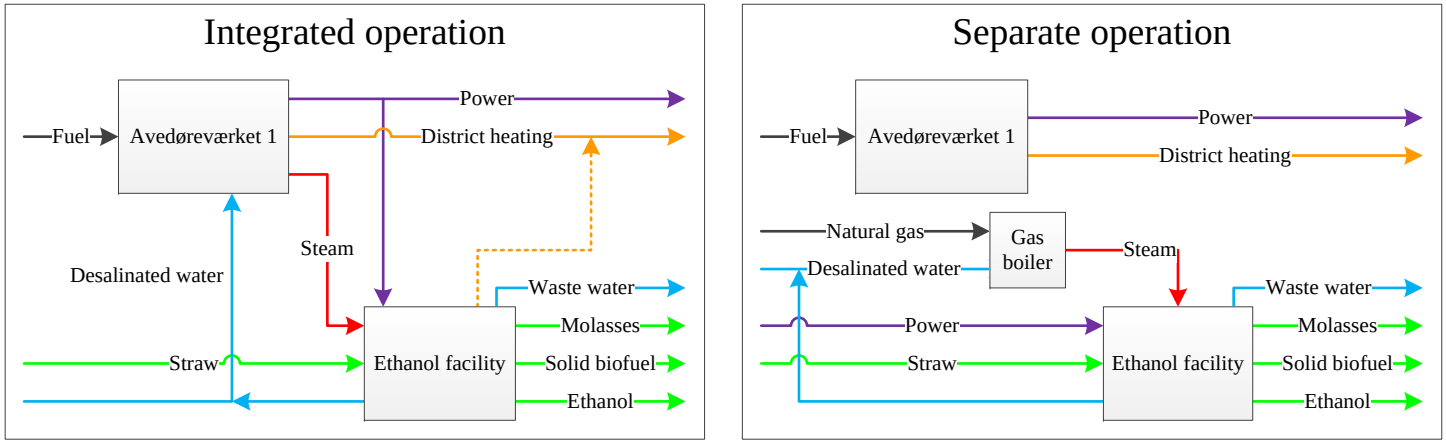
Integrated operation
Fuel
Avedøreværket 1
Power
District heating
Steam
Desalinated water
Waste water
Molasses
Straw
Ethanol facility
Solid biofuel
Ethanol
Separate operation
Fuel
Avedøreværket 1
Power
District heating
Natural gas
Gas boiler
Steam
Desalinated water
Waste water
Power
Molasses
Straw
Ethanol facility
Solid biofuel
Ethanol

Figure 2 - caption

Figure 2 – Outlines of the two operation modes in the polygeneration plant. From Lythcke-Jørgensen et al. [22].

Figure 3

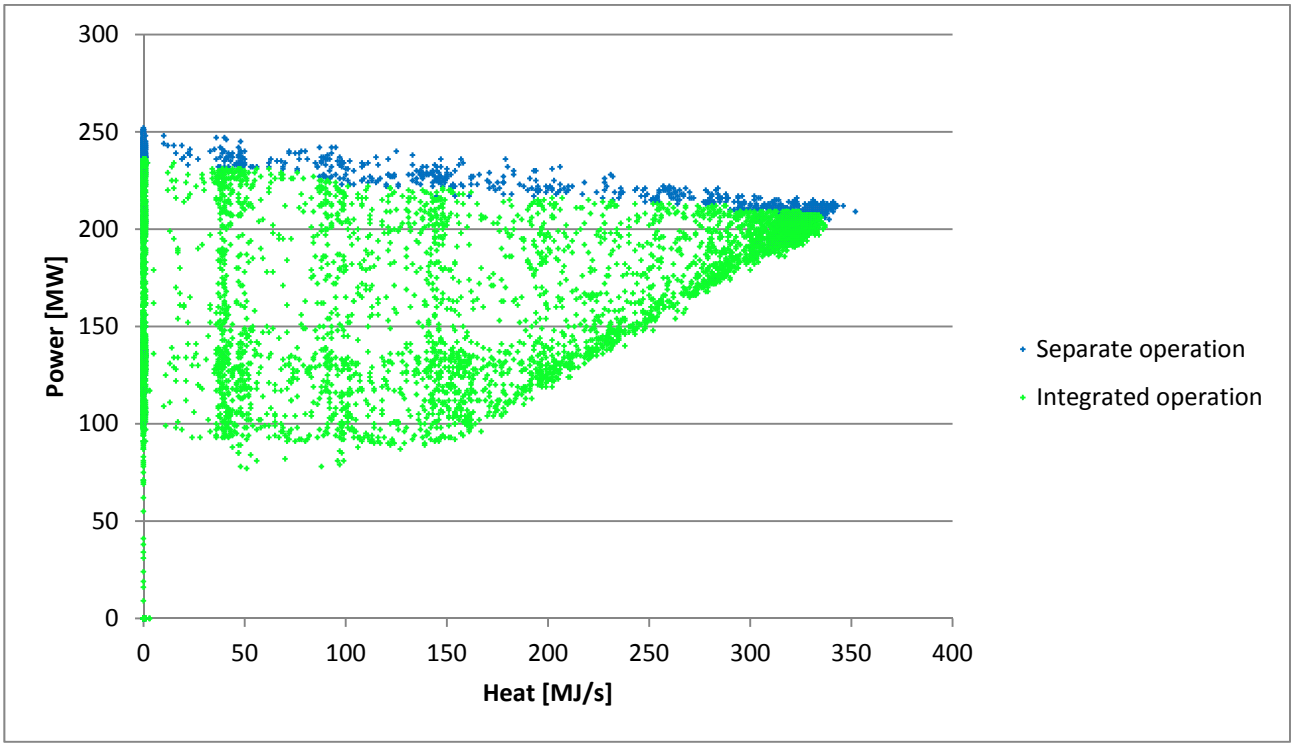
300
250
200
150
100
50
0
Power [MW]
0
50
100
150
200
250
300
350
400
Heat [MJ/s]
Separate operation
Integrated operation

Figure 3 - caption

Figure 3 – Scatter distribution of the hour-wise quasi-static operating points of the reference polygeneration plant.

Figure 4

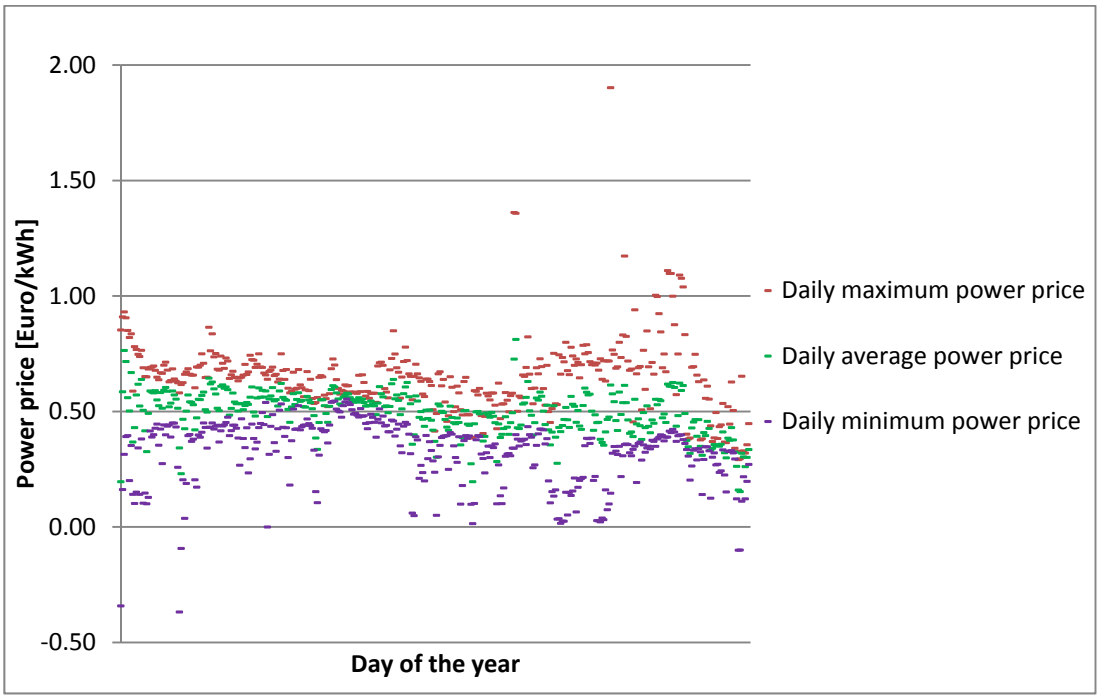
2.00
1.50
1.00
0.50
0.00
-0.50
Power price [Euro/kWh]
Day of the year
Daily maximum power price
Daily average power price
Daily minimum power price

Figure 4 - caption

Figure 4 – Scatter distribution of the daily maximum, minimum, and average electricity prices in the block 'Denmark East' in 2011.

Figure 5

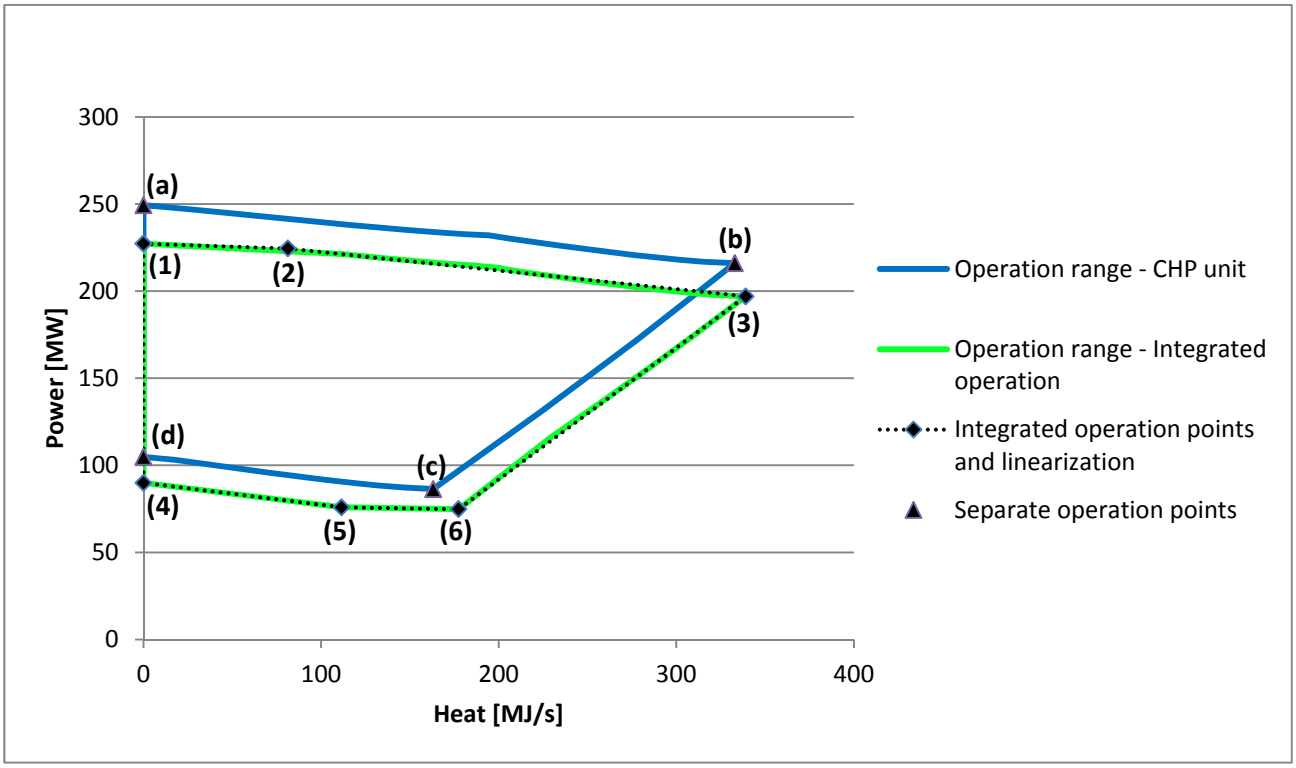
300
250
200
150
100
50
0
0
100
200
300
400
Power [MW]
Heat [MJ/s]
(a)
(b)
(c)
(d)
(1)
(2)
(3)
(4)
(5)
(6)
Operation range - CHP unit
Operation range - Integrated operation
Integrated operation points and linearization
Separate operation points

Figure 5 - caption

Figure 5 – Operational ranges for the reference PGP in integrated and separate operation.

Characteristics of the six key operation points are described in Table 6.

Figure 6

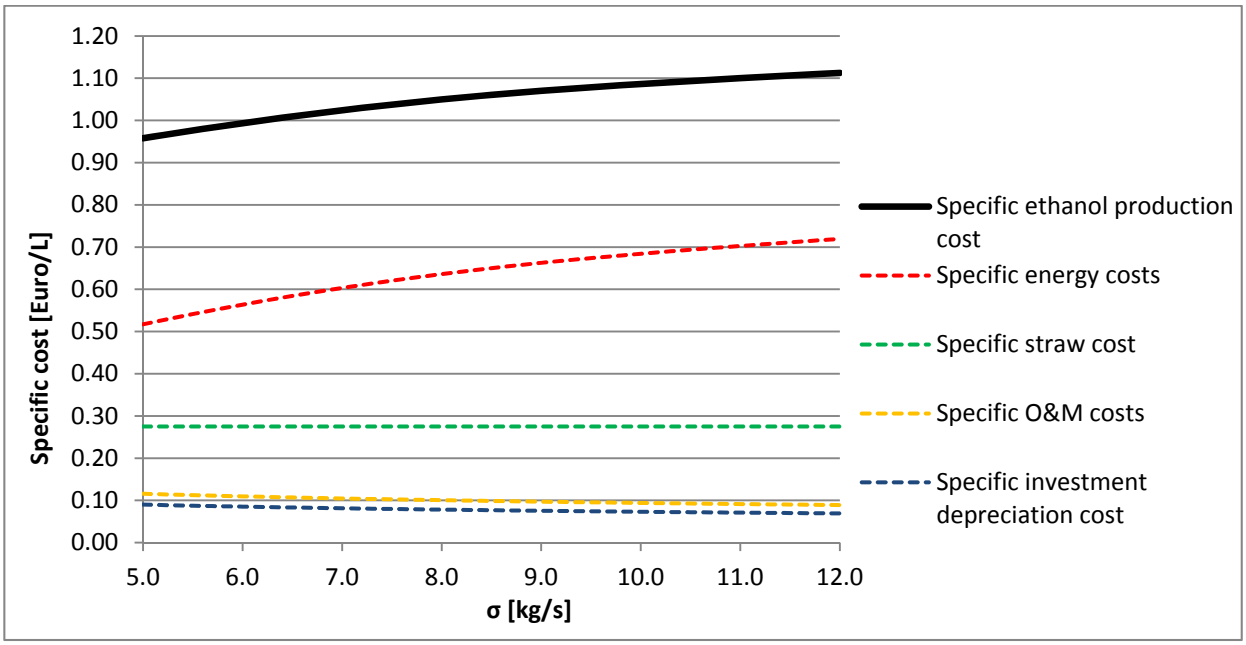
1.20
1.10
1.00
0.90
0.80
0.70
0.60
0.50
0.40
0.30
0.20
0.10
0.00
Specific cost [Euro/L]
5.0
6.0
7.0
8.0
9.0
10.0
11.0
12.0
σ [kg/s]
Specific ethanol production cost
Specific energy costs
Specific straw cost
Specific O&M costs
Specific investment depreciation cost

Figure 6 - caption

Figure 6 – Specific ethanol production cost and important cost components as functions of σ.

Figure 7

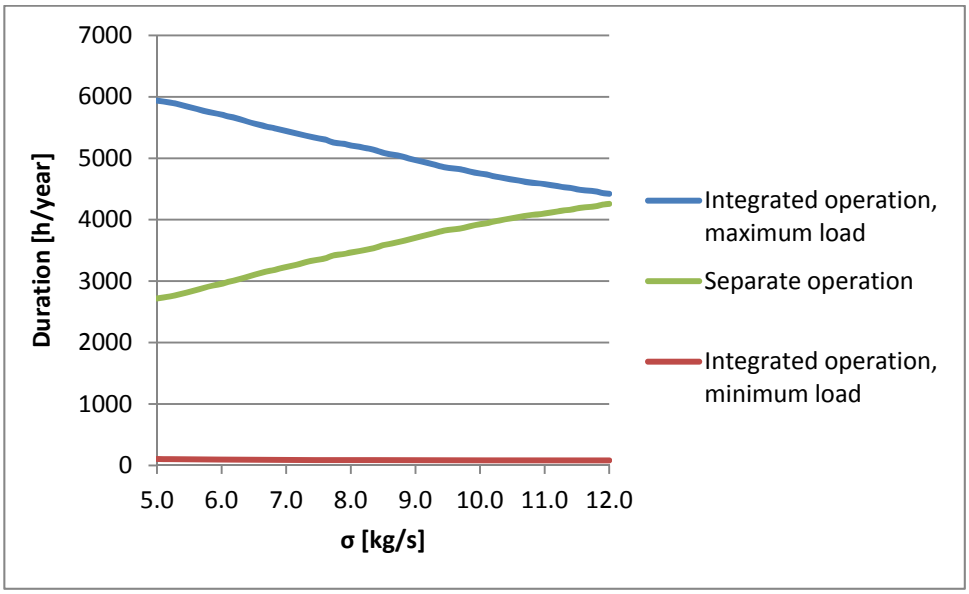
7000
6000
5000
4000
3000
2000
1000
0
Duration [h/year]
5.0
6.0
7.0
8.0
9.0
10.0
11.0
12.0
σ [kg/s]
Integrated operation, maximum load
Separate operation
Integrated operation, minimum load

Figure 7 - caption

Figure 7 – Duration of integrated and separate operation of the optimized polygeneration plant as a function of σ.

Figure 8

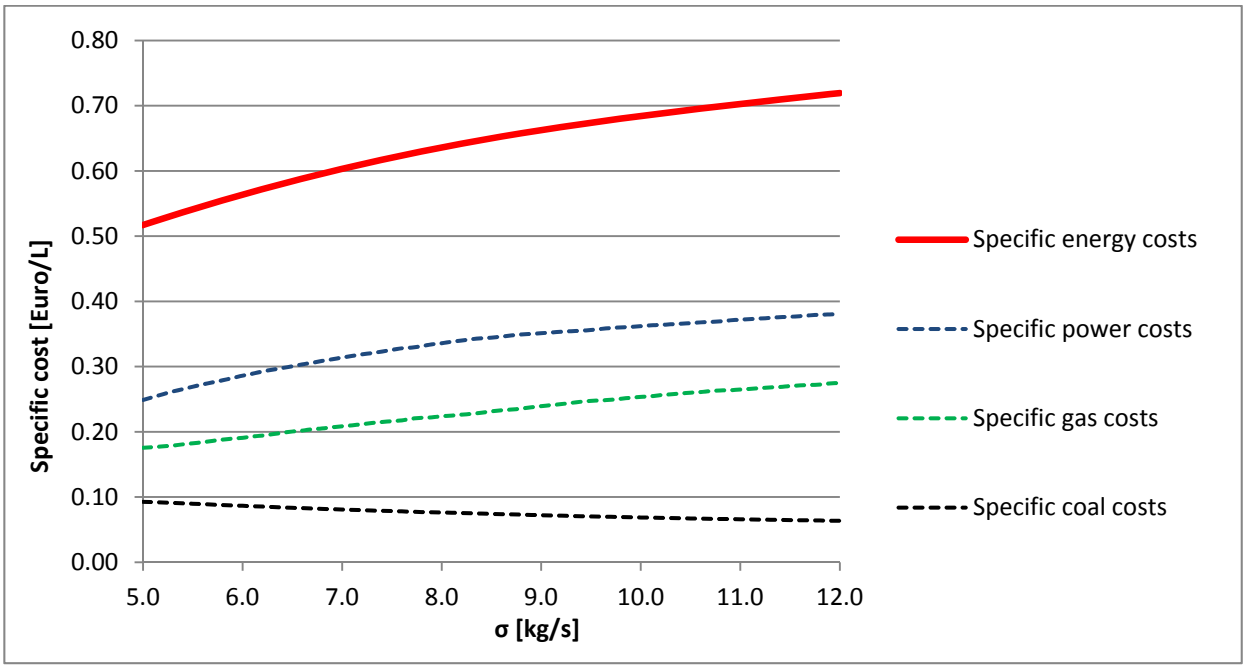
0.80
0.70
0.60
0.50
0.40
0.30
0.20
0.10
0.00
Specific cost [Euro/L]
5.0
6.0
7.0
8.0
9.0
10.0
11.0
12.0
σ [kg/s]
Specific energy costs
Specific power costs
Specific gas costs
Specific coal costs

Figure 8 - caption

Figure 8 – Components of the specific energy cost as functions of σ.

Figure 9

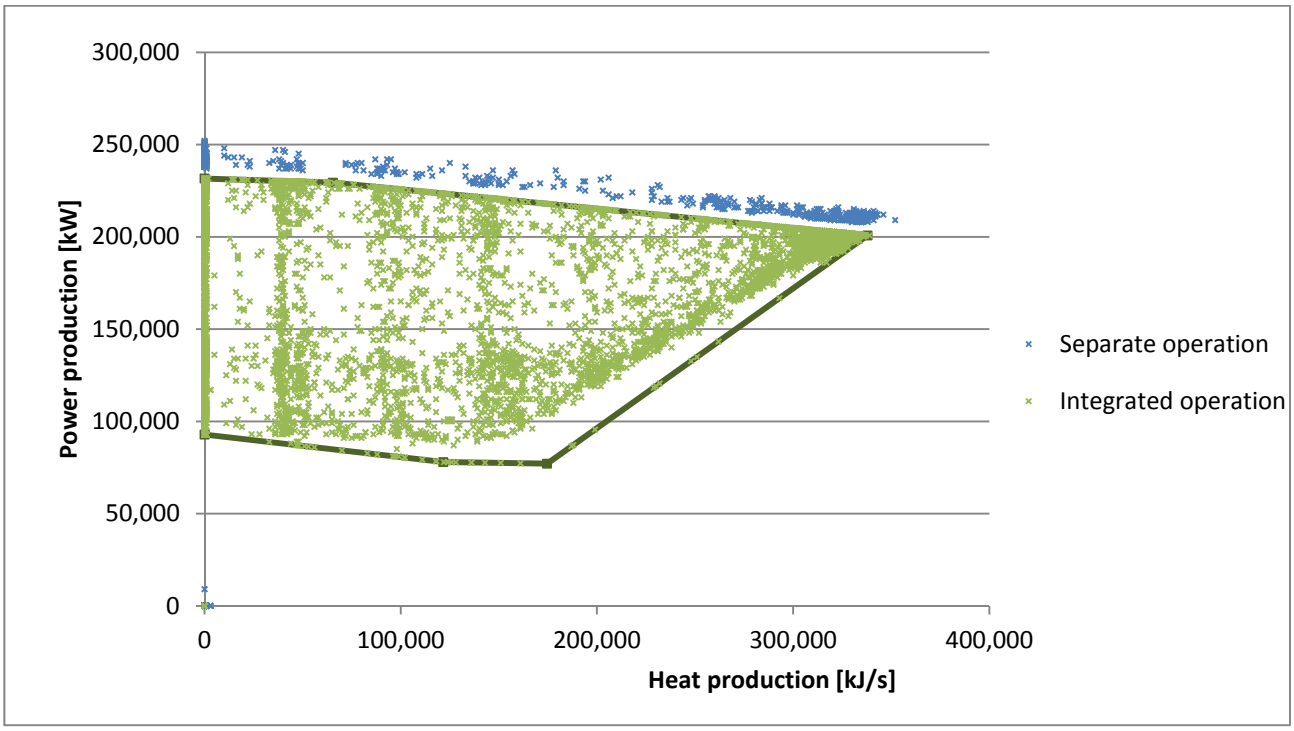
300,000
250,000
200,000
150,000
100,000
50,000
0
Power production [kW]
0
100,000
200,000
300,000
400,000
Heat production [kJ/s]
Separate operation
Integrated operation

Figure 9 - caption

Figure 9 – Scatter distribution of hour-wise quasi-static operating points for the optimal solution.

Figure 10

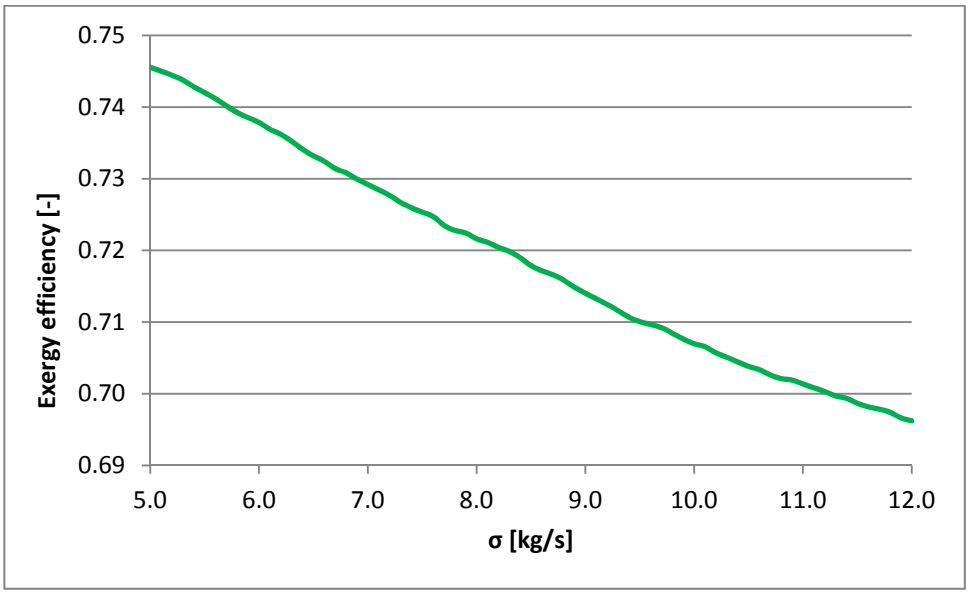
0.75
0.74
0.73
0.72
0.71
0.70
0.69
Exergy efficiency [-]
5.0
6.0
7.0
8.0
9.0
10.0
11.0
12.0
σ [kg/s]

Figure 10 - caption

Figure 10 – Yearly average exergy efficiency of the ethanol production at optimized operation pattern for various σ.

Figure 11

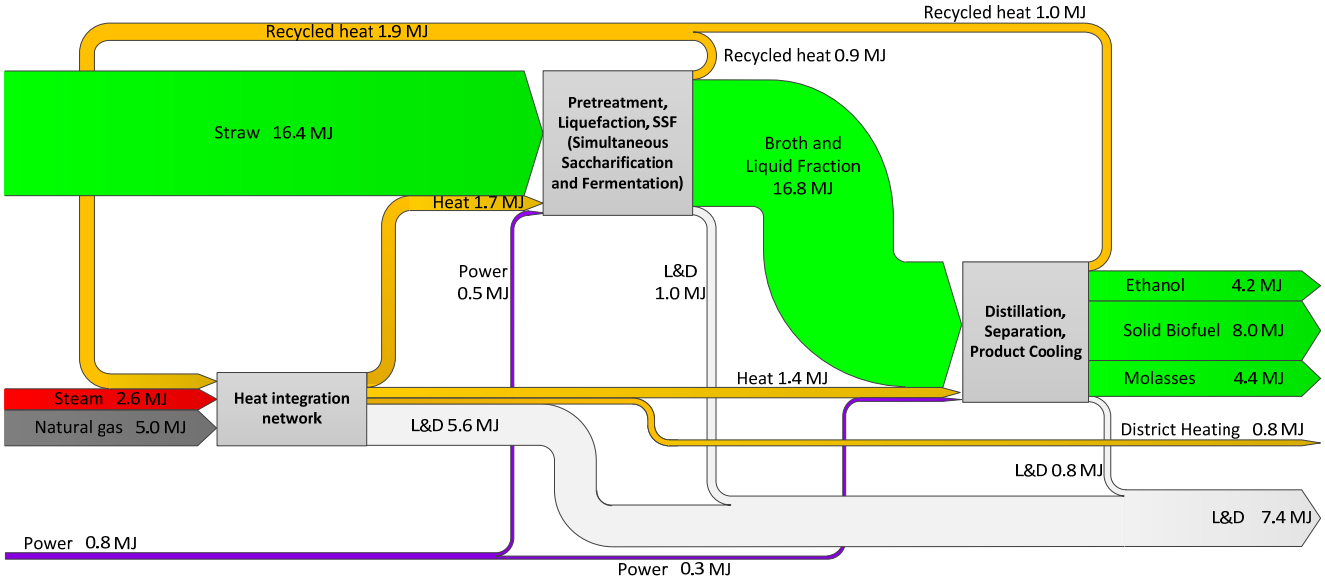
Recycled heat 1.0 MJ
Recycled heat 1.9 MJ
Recycled heat 0.9 MJ
Straw 16.4 MJ
Pretreatment, Liquefaction, SSF (Simultaneous Saccharification and Fermentation)
Broth and Liquid Fraction 16.8 MJ
Heat 1.7 MJ
Power 0.5 MJ
L&D 1.0 MJ
Distillation, Separation, Product Cooling
Ethanol 4.2 MJ
Solid Biofuel 8.0 MJ
Molasses 4.4 MJ
Heat 1.4 MJ
Steam 2.6 MJ
Natural gas 5.0 MJ
Heat integration network
L&D 5.6 MJ
District Heating 0.8 MJ
L&D 0.8 MJ
L&D 7.4 MJ
Power 0.8 MJ
Power 0.3 MJ

Figure 11 - caption

Figure 11 – Grassmann diagram illustrating yearly average exergy flows in the ethanol production for the optimal solution.

Figure 12

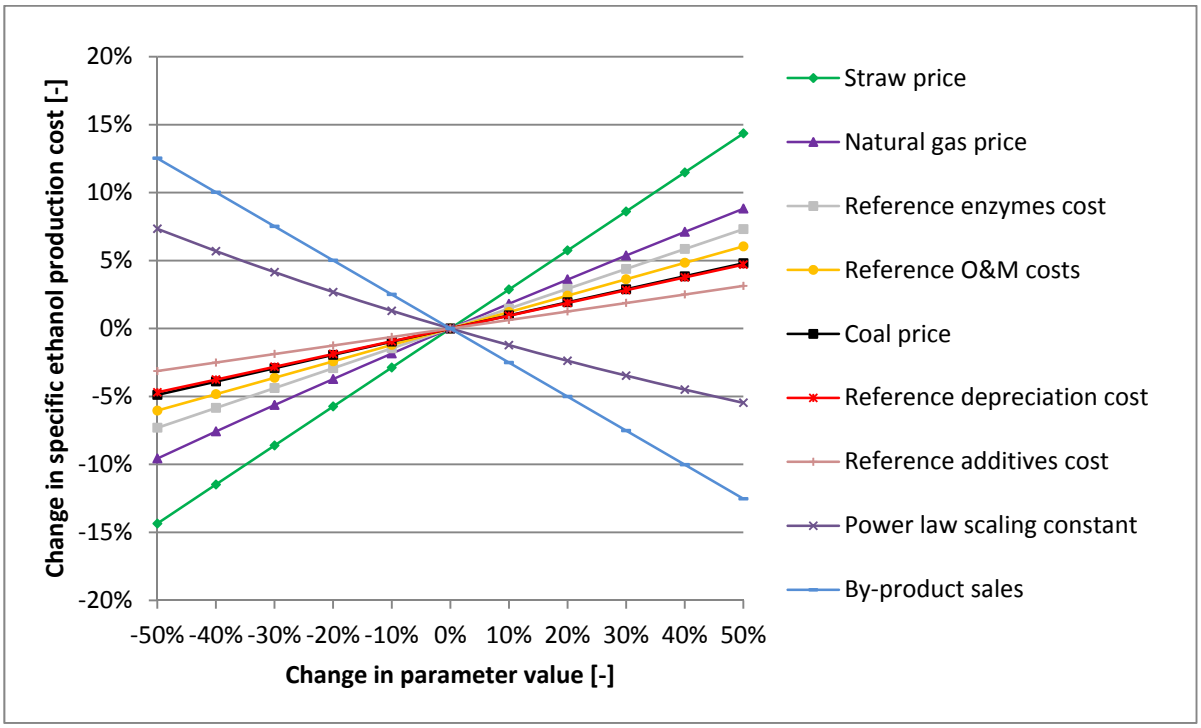
Change in specific ethanol production cost [-]
20%
15%
10%
5%
0%
-5%
-10%
-15%
-20%
-50% -40% -30% -20% -10% 0% 10% 20% 30% 40% 50%
Change in parameter value [-]
Straw price
Natural gas price
Reference enzymes cost
Reference O&M costs
Coal price
Reference depreciation cost
Reference additives cost
Power law scaling constant
By-product sales

Figure 12 - caption

Figure 12 – Spider plot showing the impact on specific ethanol production cost from varying important parameters.